*Progress In Electromagnetics Research C, Vol. 53, 165–175, 2014*

# Target Recognition with Radar Images via Parameterized Dictionary Sets

**Dang-Wei Wang*, Wen-Kun Gu, Shang Peng, and Xiao-Yan Ma**

**Abstract**—Target recognition through the processing of high-resolution radar images has been an active research area in past decades. In this paper, dictionary sets parameterized by the two-dimensional (2-D) location parameters of main high-energy scatterers are considered to recognize the candidate targets. For this purpose, the scatterer extraction and orientation estimation of radar image are firstly provided in this paper. Furthermore, the recognition method based on the parameterized dictionary sets is subsequently proposed. Different from the existed recognition methods, only the sampled images at the 2-D location parameters of main high-energy scatterers are used in the proposed method. Consequently, the noise or clutter outside the sampling locations can be filtered, which results in more robust performance. Moreover, the 2-D location parameters are proportional to the geometrical structure, and the proposed method is adaptive to the scale variation of the target images. Simulated results are provided to demonstrate the proposed method.

## 1. INTRODUCTION

Inverse synthetic aperture radar (ISAR) is an effective high resolution radar system which can provide two-dimensional (2-D) radar image of a maneuvering target like aircraft [1–3]. Two-dimensional (2-D) radar image is directly related to the geometrical structure of an interest target, and the 2-D distribution of its high energy scatterers represents the geometrical shape.

Since more direct electromagnetic information can be presented by the 2-D radar image in contrast to the one-dimensional (1-D) scattering signature, target recognition with the ISAR images has been an active research area in past decades [4–7]. As one popular method, moments of an image are often used to recognize interest targets since they are independent of the rotation and translation on the imaging plane [4]. However, moments of an image may cause a loss of discriminative information [5], and the moments-based methods are generally associated with an important assumption, such as the unchanged image intensity [8]. Therefore, the recognition performance of the method could be significantly degraded in an actual situation when the intensity of an ISAR image is changed by the possible image blurring from the invalid motion compensation. Despite the moments-based method, there still exist other recognition methods in [5–7]. The ISAR image is often transformed into a special domain such as polar mapping domain [5, 6] or 2D wavelet transform domain [7], all of which are global features of images. In these methods, the whole radar image including the location and amplitude of all scatterers on it, is used. Consequently, the feature templates at many aspect angles have to be stored beforehand to confront the aspect-dependent amplitude for fine recognition accuracy.

Recently, the local features involved in radar images have received more active attention [9–13]. In [9], the local non-negative matrix factorization from the feature space is considered to recognize the ISAR image. In [10], some information embedded in the statistical model is presented to recognize interest targets on the synthetic aperture radar (SAR) image. In [11–13], the scatterers on the SAR or ISAR image are also attempted to realize the recognition task. In general, the local features in the above

*Received 18 May 2014, Accepted 7 August 2014, Scheduled 29 September 2014*
* Corresponding author: Dang-Wei Wang (wdwjane@tom.com).
The authors are with the Wuhan Radar Academy, Wuhan 430019, China.

methods economically represent the radar images of interest targets. The recognition methods based on these features can be less sensitive to non-ideal factors such as noise or image blurring. However, in the recognition application based ISAR images, two key issues have to be considered. The first one is that the geometrical shapes of the interest ISAR targets are so similar that statistical models in [9, 10] cannot be distinguished for successful recognition. The second one is that the scatterer extraction can be a time-consuming procedure due to the prohibitively large dimension of an ISAR image. Large computation burden is unavoidable embedded in the recognition methods in [11–13] for extracting the scatterers and matching them to the stored templates.

Considering these facts, the dictionaries parameterized by the 2-D location parameters of main high-energy scatterers are proposed in this paper as the feature set for target recognition. The key issue of the proposed feature is that only 2-D location parameters of main high-energy scatterers are used, regardless of the amplitude information or scattering matrix of the radar image. Unlike the existing features [4–7], the 2-D location parameters of main high-energy scatterers on an ISAR image provide the image with very sparse representations and illuminate the scattering model of a target. Furthermore, the scattering model is often proportionately changed with the target scale and remains more stable over the wide angular region than the scatterer's amplitude [11–14]. Therefore, 2-D location parameters of main high-energy scatterers can be less sensitive to the variations of the ISAR image and more robust for target recognition. Main contribution of the proposed method in this paper is that target recognition is carried out with the parameterized dictionary set of every target and avoids the online scatterer extraction as the methods in [11–13]. Furthermore, the decomposition procedures involved in the proposed method only use the local image at the 2-D location parameters of main high-energy scatterers, and the image outside the scatterer locations is filtered out, which results in good generalization performance against noise or clutter. In addition, the parameterized dictionaries can be constructed beforehand in a more robust manner, such as the usage of a scaled target, due to the proportionate merit of the scattering model.

The remainder of the text is organized as follows. In Section 2, the scatterer extraction and orientation estimation of radar image is presented. In Section 3, the parameterized dictionary set is firstly defined, Then, the recognition method based on the dictionary set is proposed. In Section 4, numerical examples are provided to evaluate the proposed method. Finally, conclusions are summarized in Section 5.

## 2. SCATTER EXTRACTION AND ORIENTATION ESTIMATION

Generally, an ISAR image represents the target's geometry structure projected onto the 2D down-range cross-range plane. Since some locations on the target provide stronger scattering energy toward the observation aspect after the target is illuminated by an electromagnetic (EM) wave, the ISAR image of an interest target is often modeled as the summation echoes from a finite number of high-energy scattering centers. According to [3], the parameterized expression can be given by

$$I(x,y) = \sum_{n=1}^{N} A_n h\left(x - x_n,\, y - y_n\right) \tag{1}$$

where $A_n$ is the complex amplitude, $(x_n,\, y_n)$ the 2-D parameter pair of the $n$th scatterer, $N$ the number of main high-energy scatterers, and $h(x,\, y)$ is called the point spread function (PSF). In particular, according to [3], PSF can be written into

$$h\left(x,\, y\right) = \zeta \mathrm{sinc}\left(\frac{2B}{c}x\right) \mathrm{sinc}\left(\frac{2f_c\Omega}{c}y\right) \tag{2}$$

where $\zeta$ is complex amplitude, $c$ the speed of electromagnetic wave, $f_c$ the carrier frequency, and $B$ and $\Omega$ are the frequency bandwidth and the observation angle width, respectively.

According to the scattering model, 2-D parameter pairs of main high-energy scatterers can drive the prediction of some image features including the target's pose and geometrical shape, which implies that the target's pose or image orientation can be estimated by 2-D parameter pairs of main high-energy scatterers. In this subsection, the approaches about the scatter extraction and orientation estimation are presented, respectively.

### 2.1. Scatterer Extraction

In general, the scatterer extraction of the radar image can be carried out by the algorithms in [3–16]. In [16], the matching pursuits (MP) algorithm is used to extract the parameters of main high-energy scatterers for the recognition application. At each iteration in the algorithm, the dictionary atom like expression (2) is assigned with the variational location parameters and moved throughout the whole radar image. When the inner product between the dictionary atom and the radar image reaches its maximum value, the parameter pair of one scatterer is extracted. With the increase of the iteration, main scatterers can be extracted one by one. Let the inner product between the image $I(x, y)$ and the atom $\varphi_{ij}(x - x_i, y - y_j)$ be defined as

$$\langle I, \varphi_{ij} \rangle = \int_{-\infty}^{+\infty} I(x, y) \varphi_{ij}^{*}(x - x_i, y - y_j) dx \tag{3}$$

where superscript $*$ denotes complex conjugate, and the atom $\varphi_{ij}(x - x_i, y - y_j)$ satisfies $\|\varphi_{ij}\|^2 = 1$. Specially, the atom $\varphi_{ij}(x - x_i, y - y_j)$ can be given by

$$\varphi_{ij}(x - x_i, y - y_j) = \alpha \operatorname{sinc}\left[\frac{2B}{c}(x - x_i)\right] \operatorname{sinc}\left[\frac{2f_c\Omega}{c}(y - y_j)\right] \tag{4}$$

where $\alpha$ is a the energy-normalized coefficient, and the parameter pair $(x_i, y_j)$ is the assigned atom center. To traverse the whole image, the atom center should be assigned with the pixel coordinates of the radar image.

Then, the $n$th scatterer is extracted only when the relationship is satisfied with

$$I(x, y) = \sum_{n'=0}^{n} \left\langle R^{(n')} I, \varphi_{ij}^{(n')} \right\rangle + R^{(n+1)} I \tag{5}$$

where $R^{(n+1)}I$ denotes the residual after $n$ iterations, which is given by

$$R^{(n+1)} I = I(x, y) - \sum_{n'=0}^{n} \left\langle R^{(n')} I, \varphi_{ij}^{(n')} \right\rangle \varphi_{ij}^{(n')}(x - x_i, y - y_j) \tag{6}$$

where $R^{(0)}I = I(x, y)$ and $|\langle R^{(n')}I, \varphi_{ij}^{(n')}\rangle| \geq |\langle R^{(n')}I, \varphi_{ij}\rangle|$.

Following the properties of the MP algorithm, the above iteration procedure can extract the scatterers whose energy values descend with the increasing of the iteration number. Therefore, one might set a fine iteration number to terminate the algorithm and extract main high-energy scatterers.

### 2.2. Orientation Estimation

Image orientation is helpful for reducing the search scope in the recognition procedure and is often described by the direction of the radar line of sight (LOS). To illuminate the presented method, let us define the image orientation as the rotation angle away from the right direction of the $x$-axis, i.e., the azimuth angle $\phi$ displayed in Fig. 1. Furthermore, we also assume that $S^{(m)} = \left\{ \left( \bar{x}_{ij}^{(m)}, \bar{y}_{ij}^{(m)} \right) | i = 1, 2, \ldots, N_m; j = 1, 2, \ldots, M \right\}$ denotes the stored template set of the $m$th target, where the parameter template $(\bar{x}_{ij}^{(m)}, \bar{y}_{ij}^{(m)})$ of the $i$th scattering center is extracted from the image at elevation angle $\theta_j$. A typical architecture of the stored template set of the $m$th target is shown in Fig. 2. In particular, the elevation angle $\theta_j$ represents the angle formed by a unit vector orthogonal to the radar LOS and the cross-range plane. That is to say, $S^{(m)}$ almost includes all possible scatterer parameters of a three-dimensional (3-D) target body when $\theta_j$ is varied from 0 to $2\pi$ with a right angular interval, i.e., not beyond 3° [17]. Consequently, a zero-centered image $I(x, y)$ sampled at the parameter template $(\bar{x}_{ij}^{(m)}, \bar{y}_{ij}^{(m)})$ can be expressed as

$$\bar{I}\left( \bar{x}_{ij}^{(m)}, \bar{y}_{ij}^{(m)} \right) = \iint \delta\left( x - \bar{x}_{ij}^{(m)}, y - \bar{y}_{ij}^{(m)} \right) I(x, y) dxdy \tag{7}$$

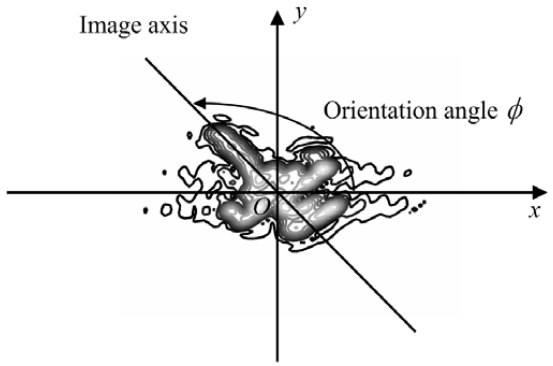


**Figure 1.** Orientation definition of the radar image.

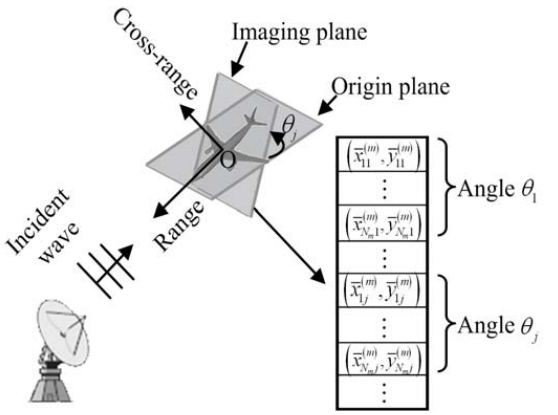


**Figure 2.** Typical architecture of the stored template set.

where $\delta(\cdot)$ is a 2-D Dirichlet function with unit energy.

Furthermore, let us define the inertia of the sampled image as

$$J_j^{(m)} = \sum_i \left(\bar{x}_{ij}^{(m)} \sin\phi - \bar{y}_{ij}^{(m)} \cos\phi\right)^2 \bar{I}\left(\bar{x}_{ij}^{(m)}, \bar{y}_{ij}^{(m)}\right) \quad j = 1, 2, \ldots, M \tag{8}$$

According to [18], if let $\phi_0$ denote the orientation angle of the sample image $\bar{I}(\bar{x}_{ij}^{(m)}, \bar{y}_{ij}^{(m)})$, the inertia will reach its minimum value only when $\phi$ is equal to $\phi_0$, and the minimum inertia of the sampled image can be given by

$$J_{\min}^{(m)} = \min_j \left[\sum_i \left(\bar{x}_{ij}^{(m)} \sin\phi_0 - \bar{y}_{ij}^{(m)} \cos\phi_0\right)^2 \bar{I}\left(\bar{x}_{ij}^{(m)}, \bar{y}_{ij}^{(m)}\right)\right] \tag{9}$$

That is to say, one might estimate the orientation of the sampled image with its minimum inertia, but the large estimation error an happen to the whole image $I(x, y)$ when the parameter template $(\bar{x}_{ij}^{(m)}, \bar{y}_{ij}^{(m)})$ mismatches the real orientation of the whole image. Therefore, one must perform an additional procedure.

Let us axial-rotate the parameter template $(\bar{x}_{ij}^{(m)}, \bar{y}_{ij}^{(m)})$ by the angle $\varphi$ to produce a different template $(\bar{x}_{ij}^{'(m)}, \bar{y}_{ij}^{'(m)})$, where

$$\begin{cases} \bar{x}_{ij}^{'(m)} = \bar{x}_{ij}^{(m)} \cos\varphi - \bar{y}_{ij}^{(m)} \sin\varphi \\ \bar{y}_{ij}^{'(m)} = \bar{x}_{ij}^{(m)} \sin\varphi + \bar{y}_{ij}^{(m)} \cos\varphi \end{cases} \tag{10}$$

and resample the image $I(x, y)$ with the template $(\bar{x}_{ij}^{'(m)}, \bar{y}_{ij}^{'(m)})$ to obtain the image $\bar{I}'(\bar{x}_{ij}^{'(m)}, \bar{y}_{ij}^{'(m)})$. According to expression (9), the minimum inertia of the resampled image can be given by

$$J_{\min}^{'(m)} = \min_j \left\{\sum_i \left[\bar{x}_{ij}^{'(m)} \sin(\phi_0 + \varphi) - \bar{y}_{ij}^{'(m)} \cos(\phi_0 + \varphi)\right]^2 \bar{I}'\left(\bar{x}_{ij}^{'(m)}, \bar{y}_{ij}^{'(m)}\right)\right\} \tag{11}$$

Following the Cauchy-Schwarz inequality in [19], one might obtain the relationship as

$$\left|J_{\min}^{'(m)}\right| \le \min_j \left[L\left(\bar{x}_{ij}^{'(m)}, \bar{y}_{ij}^{'(m)}\right) \cdot E\left(\bar{x}_{ij}^{'(m)}, \bar{y}_{ij}^{'(m)}\right)\right] \tag{12}$$

where

$$L\left(\bar{x}_{ij}^{'(m)}, \bar{y}_{ij}^{'(m)}\right) = \sum_i \left[\bar{x}_{ij}^{'(m)} \sin(\phi_0 + \varphi) - \bar{y}_{ij}^{'(m)} \cos(\phi_0 + \varphi)\right]^2 \tag{13}$$

$$E\left(\bar{x}_{ij}^{'(m)}, \bar{y}_{ij}^{'(m)}\right) = \sum_i \left|\bar{I}'\left(\bar{x}_{ij}^{'(m)}, \bar{y}_{ij}^{'(m)}\right)\right| \tag{14}$$

Since $L(\bar{x}_{ij}^{'(m)}, \bar{y}_{ij}^{'(m)})$ can be seen as the minimum inertia of a binary image whose amplitude at the coordinate $(\bar{x}_{ij}^{'(m)}, \bar{y}_{ij}^{'(m)})$ is equal to one or zero at other coordinates, the value of $L(\bar{x}_{ij}^{'(m)}, \bar{y}_{ij}^{'(m)})$ is independent of the sampled image $\bar{I}'(\bar{x}_{ij}^{'(m)}, \bar{y}_{ij}^{'(m)})$.

Furthermore, according to the property of the minimum inertia, one might obtain

$$L\left(\bar{x}_{ij}^{'(m)}, \bar{y}_{ij}^{'(m)}\right) = \sum_i \left(\bar{x}_{ij}^{(m)} \sin\phi_0 - \bar{y}_{ij}^{(m)} \cos\phi_0\right)^2 \tag{15}$$

That is to say, $L(\bar{x}_{ij}^{'(m)}, \bar{y}_{ij}^{'(m)})$ is invariant to rotation and always keeps a constant value for any rotation angle $\varphi$. Therefore, $|J_{\min}^{'(m)}|$ can reach its maximum only when $E(\bar{x}_{ij}^{'(m)}, \bar{y}_{ij}^{'(m)})$ is maximized by $(\bar{x}_{ij}^{'(m)}, \bar{y}_{ij}^{'(m)})$ at special rotation angle $\varphi$ and right elevation angle $\theta_j$. Fortunately, maximizing $|J_{\min}^{'(m)}|$ is very possible for many aerial targets, e.g., planes and missiles because the targets are often regular and symmetric, but not circularly symmetric. For these targets, $E(\bar{x}_{ij}^{'(m)}, \bar{y}_{ij}^{'(m)})$ can reach its maximum value when the orientation axis of the sampled image overlaps the axis of the original image. Therefore, the orientation of the radar image can be estimated via calculating the minimum inertia of the sampled image with the maximum energy.

In addition, it must be pointed out that three key issues must be considered for the successful orientation estimation of the image of a three-dimensional (3-D) target. The first one is that the azimuth angle $\varphi$ in the previous orientation estimation has to be rotated discretely from 0 to $2\pi$ with a special interval to find the azimuth angle of the image $I(x, y)$ with the parameter template $(\bar{x}_{ij}^{(m)}, \bar{y}_{ij}^{(m)})$ at elevation angle $\theta_j$. The second one is that the estimation procedure should be carried out for all scatterer templates of every target to locate the right elevation angle. The third one is that the orientation estimation should be also used to all scatterer templates of all targets in the target database because the class of the image $I(x, y)$ is unknown before the recognition procedure. Consequently, the orientation angles estimated from the image $I(x, y)$ can be different for candidate targets, but the matched scatterer template can be indicated for every target.

## 3. PROPOSED RECOGNITION METHOD

The dictionary set is a classifiable feature which has been used to recognize a candidate target through the processing of the 1-D scattering signatures of a target in [20, 21]. As shown in [20], the extracted dictionary can ensure the smallest representation error when target matches its dictionary set and the worst error when target mismatches its dictionary set. Inspired by the existing methods, this paper focuses attention on developing the recognition method of the 2-D radar image via the dictionary set parameterized by the location parameters of main high-energy scatterers.

### 3.1. Construction of Dictionary Set

Different from the dictionaries used in [20–22], the dictionary set in this paper is built up with the 2-D scatterer parameter of radar images. Let $\mathbf{\Gamma}^{(m)} = \{\mathbf{\Phi}_j^{(m)}, j = 1, 2, \ldots, M\}$ denote the dictionary set with $M$ dictionaries and $\mathbf{\Phi}_j^{(m)} = \left\{\psi_{ij}^{(m)}(x, y), i = 1, 2, \ldots, N_m\right\}$ denote its $j$th dictionary, whose atom $\psi_{ij}^{(m)}(x, y)$ is defined as

$$\psi_{ij}^{(m)}(x, y) = \alpha \text{sinc}\left[\frac{2B}{c}\left(x - \hat{x}_{ij}^{(m)}\right)\right] \text{sinc}\left[\frac{2f_c\Omega}{c}\left(y - \hat{y}_{ij}^{(m)}\right)\right] \tag{16}$$

where $\left(\hat{x}_{ij}^{(m)}, \hat{y}_{ij}^{(m)}\right)$ denotes the found scatterer parameter of the $m$th target after the orientation estimation. If assume that $\hat{\phi}_0^{(m)}$ is the orientation angle estimated by the stored scatterer template of the $m$th target, one might use the expression in (10) to rotate the stored template $\left(\bar{x}_{ij}^{(m)}, \bar{y}_{ij}^{(m)}\right)$ with the angle $\hat{\phi}_0^{(m)}$ and to calculate the parameter $\left(\hat{x}_{ij}^{(m)}, \hat{y}_{ij}^{(m)}\right)$.

Furthermore, the energy of a scatterer on the image is often assembled into a small 2-D neighborhood with the parameter $\left(\hat{x}_{ij}^{(m)}, \hat{y}_{ij}^{(m)}\right)$ as the center, and the neighborhood size is limited jointly by the range and cross-range resolutions. Therefore, one might reduce the calculation complexity of the recognition procedure via restricting the atom size with the variables $x$ and $y$. In this paper, $x$ and $y$ in the atom $\psi_{ij}^{(m)}(x, y)$ fall into the following intervals

$$x \in \left[\hat{x}_{ij}^{(m)} - 5\Delta_x, \hat{x}_{ij}^{(m)} + 5\Delta_x\right] \tag{17}$$

$$y \in \left[\hat{y}_{ij}^{(m)} - 5\Delta_y, \hat{y}_{ij}^{(m)} + 5\Delta_y\right] \tag{18}$$

where $\Delta_x$ and $\Delta_y$ are the range and cross-range resolution of the radar image, respectively.

As shown by the defined dictionary set, the dictionaries used in this paper represent the scatterer distribution of the target images associated with different aspect angles. Atom centers in the dictionary mark main scattering energy of the radar image. If angle $\theta_j$ is rightly chosen, the dictionary set can collect almost all scatterer models on a 3-D target, but be independent of the amplitude variation of the radar images.

### 3.2. Recognition Procedure

The recognition procedure in this paper is similar to the method proposed in [20]. To implement the recognition, the image $I(x, y)$ of the candidate target is decomposed with the MP algorithm in [22], where the inner product between the image $I(x, y)$ and the atom $\psi_{ij}^{(m)}(x, y)$ as

$$\left\langle I, \psi_{ij}^{(m)} \right\rangle = \int\limits_{\Omega_i^{(m)}} I(x, y)\, \psi_{ij}^{(m)}(x, y)\, dx \tag{19}$$

where $\Omega_{ij}^{(m)}$ is the support domain of the variable $x$ in the atom $\psi_{ij}^{(m)}(x, y)$.

After $N_m$ iterations, the final residual $R_{N_m}^{(m)} I(x, y)$ associated with the dictionary $\mathbf{\Phi}_j^{(m)}$ can be given by

$$R_{N_m}^{(m)} I(x, y) = I(x, y) - \sum_{i=1}^{N_m} \left\langle I, \psi_{ij}^{(m)} \right\rangle \psi_{ij}^{(m)}(x, y) \tag{20}$$

Furthermore, the residual energy can be given by

$$\left\| R_{N_m}^{(m)} I(x, y) \right\|^2 = \frac{1}{E} \iint R_{N_m}^{(m)} I(x, y)\, dxdy, \quad m = 1, 2, 3, \ldots \tag{21}$$

where $E$ denotes the energy of the image $I(x, y)$.

Since the dictionary $\mathbf{\Phi}_j^{(m)}$ characterizes the geometry shape of the $m$th target, the energy of the final residual $R_{N_m}^{(m)} I(x, y)$ can reach its minimum value when the input image is matched with the corresponding dictionary. As a result, one might recognize the image $I(x, y)$ via minimizing the residual energy in (21). Fig. 3 shows the complete procedure of the proposed recognition method, which includes three steps. In the first step, the orientation angle of the input image with the unknown class is estimated by stored scatterer templates of every target, and then, the dictionary sets are updated with the estimated orientation angles. In the second step, the MP algorithm is used to decompose the input image with the dictionary sets of targets in target database, respectively. In the third step, the input image is recognized with the minimum value of the residual energy.

Clearly, the proposed method can spatially filter out part of the image outside the scatterer template and more robust performance against the noise or clutter can be obtained than the exited recognition methods in [4–7]. Furthermore, the calculation of the scatterer templates in the dictionary avoids the online extraction in [11–13], which results in an efficient recognition procedure.

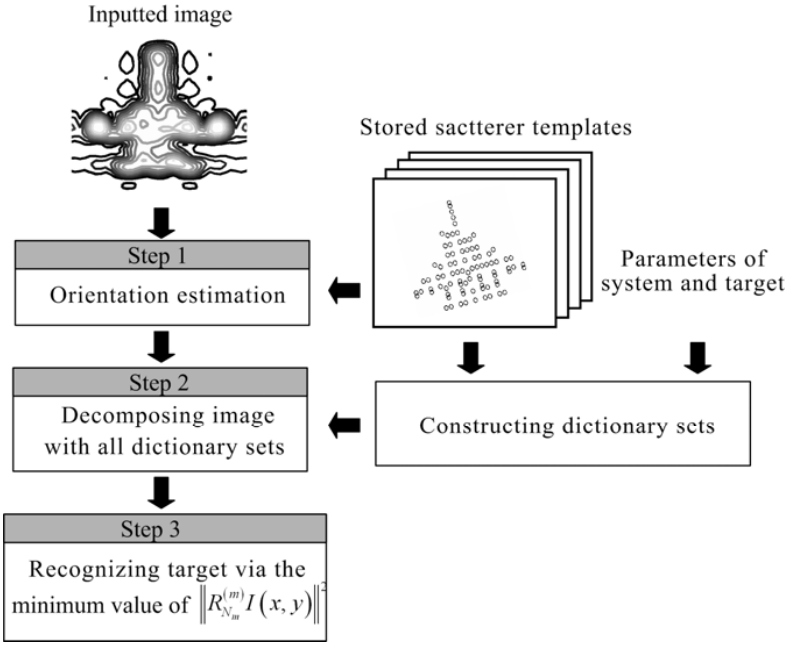


**Figure 3.** Procedure of the proposed recognition method.

## 4. SIMULATION RESULTS

To demonstrate the proposed method, the simulated radar images are used to test our method in contrast to the existing methods in [4, 5]. For the sake of notational brevity, our method will be called as "DS", the method in [4] as "IM," and the method in [5] as "PT" for all later experiments.

### 4.1. Simulation Setup

In our simulations, three aircraft targets shown in Fig. 4 are considered. The 2-D coordinates of the scatterers of every target are uniformly extracted from their geometry shapes, and the radar cross-section (RCS) of every scatterer is equal to a unit value. Furthermore, to test the recognition methods, three different databases are produced, respectively. For the first database, only axial-rotation on the imaging plane is considered to produce the images with the fixed cross-range resolution. Every target is rotated over 0°–358° aspect angles with a 2° interval to generate the scattering models at the 180 different angles while the mass center of every target is fixed at the spatial coordinate (7.765 km, 0 km,


**Figure 4.** Target geometry models used in our simulations, (a) F18; (b) F22; (c) Mig29.

28.978 km). For the second database, a scaled scene is considered. The original size of every target is reduced by a scaled coefficient value with 1/20. Furthermore, every scaled target is rotated over 0°–358° aspect angles with a 2° interval to generate 180 scatterer models with the mass center at the spatial coordinate (0 m, 0 m, 10 m). Different from the previous databases, the complex location variations are combined in the third database. The mass center of a target is moved from the spatial coordinate (7.765 km, 0 km, 28.978 km) to the spatial coordinate (30 km, 0 km, 51.962 km) with a radial-distance interval value of 5 km while every target at the given mass center is rotated over 0°–320° aspect angles with a 40° interval.

After obtaining the scattering models of three targets, Range-Doppler (RD) algorithm [3] is used to image these targets and to produce their image databases. In our simulations, the carrier frequency of the imaging system is 11.8 GHz while its bandwidth is 1.5 GHz for the second database and 150 MHz for two other databases, respectively. Furthermore, to simulate a practical situation, additional white Gaussian noise is added to the images to achieve a desired signal-noise-ratio (SNR) level. In this paper, the SNR value is measured by the maximum peak value of the image.

### 4.2. Evaluation of Scatterer Extraction and Orientation Estimation

In this experiment, we firstly extract the scatterer parameters of three targets from their radar images in the second database. For this purpose, we randomly select an image for every target from its databases and carry out the extraction procedure. Fig. 5 shows the residual energy associated with the decomposition iterations. It is seen that the residual energy reflects a slow convergence after the initial steep decay. This decline rule indicates that a relatively small number of iterations are required to represent a radar image, and the extracted scatterers locate the predominate energy on image. Therefore, one might select the iteration number within the fine region in Fig. 5 to stop the algorithm. The middle value at fine region, i.e., 86 iterations, is selected as the number of main high-energy

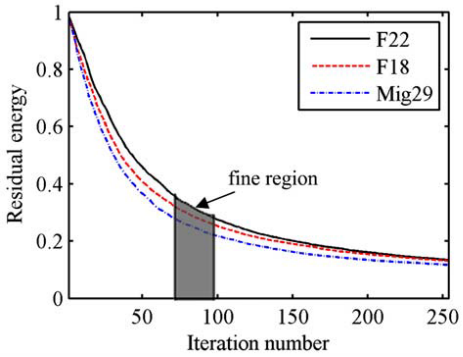


**Figure 5.** Residual energy associated with the decomposition iterations.

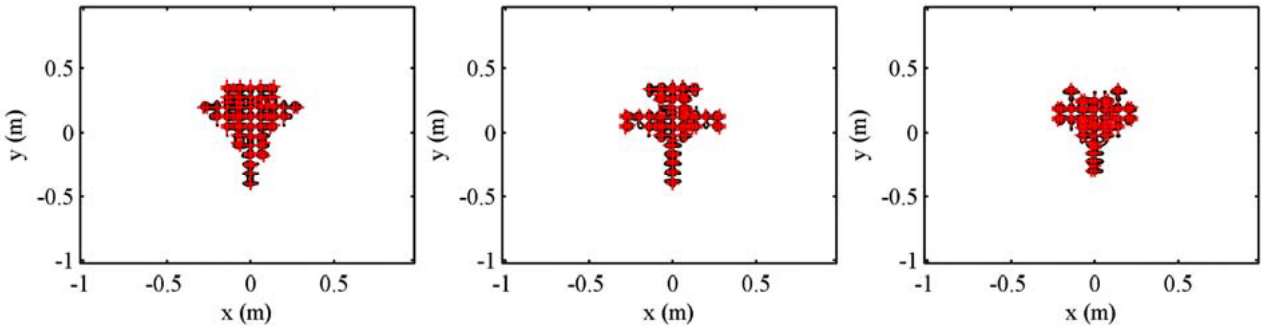


(a) F22 (b) F18 (c) Mig29

**Figure 6.** Original images and extracted scatterers of three targets.

scatterers in this paper. Furthermore, an image of every target is selected randomly from its second database, and main high-energy scatterers are extracted with 86 MP iterations. Fig. 6 shows original images and extracted scatterers for three targets. As seen in Fig. 6, the extracted scatterers coincide with the image structures of three targets and effectively characterize their geometrical shapes.

Furthermore, 86 high-energy scatterers extracted from the image are used to estimate the orientation angle. The coordinate parameters of the extracted scatterers are multiplied by 20 and axial-rotated from 0 to $2\pi$ with a $2^\circ$ interval to produce the scatterer templates for every target. Then, we randomly select the radar image of every target from its first image database with an equal probability of being present. For the selected image, scatterer templates of the corresponding target are used to estimate its orientation through 1000 experiments at a given SNR. To measure the estimation precision, the averaged estimation error is defined as the total estimation error normalized by the experiment number, where the total estimation error within 1000 experiments is the summation of the single error between the real orientation angle and the estimated angle of the selected image. Fig. 7(a) shows the averaged estimation error at different SNR values. It is seen from Fig. 7(a) that the presented method can availably estimate the orientation angle of the images. With the increase of the SNR value, the averaged estimation error values for three targets are converged to about $4.5^\circ$, $4.9^\circ$ and $2^\circ$, respectively. Moreover, we estimate the orientation of the images in the third database like the above experiment procedure, and the averaged estimation error is shown in Fig. 7(b).Similar properties are seen, and the averaged estimation error is also converged in the higher SNR condition.

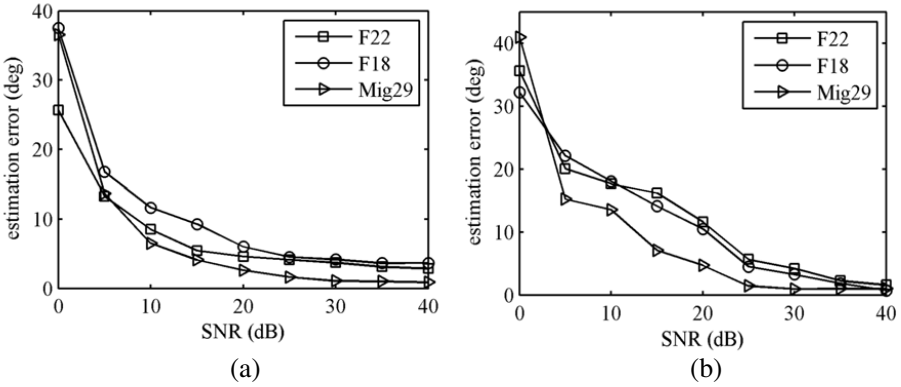


**Figure 7.** Estimation errors for the images in (a) the first database; (b) the third database.

### 4.3. Evaluation of Recognition Methods

In this experiment, three different methods, named as the "DS", "IM" and "PT", are evaluated, respectively. For this purpose, the recognition features for three methods are firstly extracted from the first image database. Especially, for the "IM' method, an image is randomly selected from the first image database of every target, and the image separated by a mean threshold in [5] is used to calculate the invariant moments as the feature vectors. For the "PT" method, the first image database of each target is uniformly sampled with the interval value of $4^\circ$ across the aspect to extract its feature vectors with the training procedure in [5]. Furthermore, for the "DS" method, the estimated orientation angles and the scatterer templates associated with three targets are to construct the corresponding dictionary sets. To test the performance of the three methods, a target is randomly selected from the target library, and an image is also selected from its first image database with an equal probability of being present. Furthermore, we carry out 1000 independent recognition tests at each given SNR value. Fig. 8(a) shows the correct recognition ratio (CRR) values of three methods. As seen in Fig. 8(a), very poor CRR value, about 33% for the simulated SNR values, is obtained by the "IM" method due to the variation of the image density. The CRR value of the "PT" method is significantly lower than that of the "DS" method within the SNR ranges from 0 dB to 16 dB although the CRR values of two methods can be close at higher SNR values. This is because a spatially filtering procedure is involved in the "DS" method, but other two methods are not so.

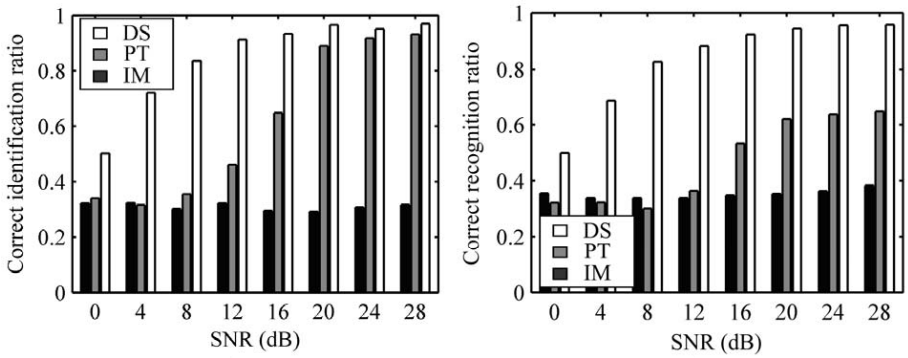


**Figure 8.** Correct recognition ratio of images, (a) in the first database; (b) in the second and third databases.

Moreover, a more challenging recognition task is carried out, where the features are extracted with the above experiments from the second image database of three targets. However, for the proposed method, the extracted location parameters of main high-energy scatterers are multiplied by 20 to match the origin target. After building up the features of three methods, we evaluate the recognition performance with the energy-normalized images in the third image database. Fig. 8(b) shows the CRR values at different SNR values, where 1000 independent tests are also carried out at a given SNR. As expected by us, the proposed method obviously outperforms other two methods. The proposed "DS" method is almost not affected by the scale variation of the target shape while the "PT" method becomes worse. In other words, the proposed method can beforehand collect the feature templates in a more robust manner.

## 5. CONCLUSIONS

Target recognition with the radar images has been a challenging task in the radar community. In this paper, main high-energy scatterers are proposed to recognize radar images via parameterized dictionary set. Furthermore, the extraction algorithm of main high-energy scatterers and the orientation estimation of radar image are presented, respectively. Simulation results show that the proposed method significantly outperforms other two methods in [4, 5] since it can counteract some difficulties associated with a radar image, e.g., the distance-dependent resolution, amplitude fluctuation, and scatterer's location rotation. Furthermore, the proposed method uses the parameterized dictionary set as the features and avoids the online extraction of the scatterers, which results in an efficient recognition procedure over the methods in [11–13].

However, it should be noted that the performance of the proposed method is evaluated only by the simulated images. The scatterers on the images are assumed solely from the geometry of the target as opposed from the actual scattering physics. Thus, the simulated results are limited in its meaning. Future work needs to particularly emphasize the performance evaluation through the measured images.

## ACKNOWLEDGMENT

The authors would like to thank the anonymous reviewers for their helpful comments and suggestions. This work was supported in part by the National Natural Science Foundation of China under Grant 61179015.

## REFERENCES

1. Zeng, B., M. D. Xing, and T. Wang, *Radar Imaging Technique*, Publish House of Electronics Industry, China, 2005.
2. Son, J. S., G. Thomas, and B. C. Flores, *Range-Doppler Radar Imaging and Motion Compensation*, Artech House, USA, 2000.

3. Özdemir, C., *Inverse Synthetic Aperture Radar Imaging with MATLAB*, John Wiley & Sons, Inc., 2012.
4. Emanuel, R., Q. Andre, and T. Felix, "Supervised self-organizing classification of superresolution ISAR images: An anechoic chamber experiment," *EURASIP Journal on Applied Signal Processing*, Vol. 2006, 1–14, Jan. 2006.
5. Kim, K. T., D. K. Seo, and H. T. Kim, "Efficient classification of ISAR images," *IEEE Transactions on Antennas and Propagation*, Vol. 53, No. 5, 1611–1621, May 2005.
6. Toumi, A. and A. Khenchaf, "Log-polar and polar image for recognition targets," *2010 IEEE International Geoscience and Remote Sensing Symposium (IGARSS)*, 1609–1612, 2010.
7. Kumar, B. S., B. Prabhakar, K. Suryanarayana, et al., "Target recognition using harmonic wavelet based ISAR imaging," *Journal of Applied Signal Processing, Special Issue on ISAR*, Vol. 2006, 1–12, Jan. 2006.
8. Patil, P. M. and J. V. Kulkarni, "Rotation and intensity invariant shoeprint matching using Gabor transform with application to forensic science," *Pattern Recognition*, Vol. 42, 1308–1317, 2009.
9. Tang, N., X.-Z. Gao, and X. Li, "Target classification of ISAR images based on feature space optimization of local non-negative matrix factorization," *IET Signal Processing*, Vol. 6, No. 5, 494–502, 2012.
10. Liu, M., Y. Wu, P. Zhang, et al., "SAR target configuration recognition using locality preserving property and Gaussian mixture distribution," *IEEE Geosci. Remote Sens. Letters*, Vol. 10, No. 2, 268–272, Mar. 2013.
11. Zhou, J. X., Z. G. Shi, X. Cheng, and Q. Fu, "Automatic target recognition of SAR images based on global scattering center model," *IEEE Trans. Geosci. Remote Sens.*, Vol. 49, No. 10, 3713–3729, Oct. 2011.
12. Martorella, M., E. Giusti, and L. Demi, "Target recognition by means of polarimetric ISAR images," *IEEE Transactions on Aerospace and Electronic Systems*, Vol. 47, No. 1, 225–239, Jan. 2011.
13. Giusti, E., M. Martorella, and A. Capria, "Polarimetrically-persistent-scatterer-based automatic target recognition," *IEEE Trans. Geosci. Remote Sens.*, Vol. 49, No. 11, 4588–4599, Nov. 2011.
14. Rao, W., G. Li, X. Wang, et al., "Adaptive sparse recovery by parametric weighted L1 minimization for ISAR imaging of uniformly rotating targets," *IEEE Journal of Selected Topics in Applied Earth Observations and Remote Sensing*, Vol. 6, No. 2, 942–952, Apr. 2013.
15. Teague, M. R., "Image analysis via the general theory of moments," *Journal of the Optical Society of America*, Vol. 70, No. 8, 920–930, Aug. 1980.
16. Wang, D.-W., G. Chen, N. Wu, et al., "Efficient target identification for MIMO high-resolution imaging radar via plane-rotation-invariant feature," *IEEE International Symposium on Signal Processing and IT*, 350–354, Ajman, UAE, 2009.
17. Bhalla, R., H. Ling, J. Moore, et al., "3D scattering center representation of complex targets using the shooting and bouncing ray technique: A review," *IEEE Antennas Propag. Mag.*, Vol. 40, No. 5, 30–39, Oct. 1998.
18. Žuni, J., L. Kopanjab, and J. E. Fieldsenda, "Notes on shape orientation where the standard method does not work," *Pattern Recognition*, Vol. 39, 856–865, 2006.
19. Gradshteyn, I. S. and I. M. Ryzhik, *Tables of Integrals, Series, and Products*, 6th Edition, Academic Press, San Diego, CA, 2000.
20. Wang, D. W., X. Y. Ma, and Y. Su, "Radar target recognition using a likelihood ratio test and matching pursuit technique," *IEE Proceedings — Radar, Sonar and Navigation*, Vol. 153, No. 6, 509–515, Dec. 2006.
21. Bharadwaj, P. K., P. Runkle, and L. Carin, "Target recognition with wave-based matched pursuits and hidden Markov models," *IEEE Transactions on Antennas and Propagation*, Vol. 47, No. 10, 1543–1554, Oct. 1999.
22. McClure, M. R. and L. Carin, "Matching pursuits with a wave-based dictionary," *IEEE Transactions on Signal Processing*, Vol. 45, No. 12, 2912–2927, Dec. 1997.